Understanding Electron Transport in Disk-Shaped Triphenylene-Tris(naphthaleneimidazole)s through Structural Modification and Theoretical Investigation

Yue Zhang,[†,‡,¥] *David A. Hanifi,*[‡,%] *M. Paz Fernández-Liencres,*[&,‡] *Liana M. Klivansky,*[†] *Biwu Ma,*[#] *Amparo Navarro,*[&*] *and Yi Liu*[†*]

[†]The Molecular Foundry and [#]Material Sciences Division, Lawrence Berkeley National Laboratory, One Cyclotron Road, Berkeley, California, 94720, USA

[%]Department of Chemistry, Stanford University, Palo Alto, California, 94305, USA

[&]Department of Physical and Analytical Chemistry, Faculty of Experimental Sciences, Universidad de Jaén, Campus Las Lagunillas, E23071 Jaén, Spain

[#]Department of Chemical & Biomedical Engineering, FAMU-FSU College of Engineering, Materials Science Program, Florida State University, Tallahassee, FL, 32310, USA

[¥]Institute of Advanced Materials (IAM), Nanjing Tech University, 30 South Puzhu Road, Nanjing 211816, China

KEYWORDS. Charge transport, columnar stacking, disk-shaped molecules, *n*-type, organic semiconductor.

ABSTRACT. Disk-shaped molecules with large aromatic π-surface are a class of organic semiconductors of which the charge carrier transport properties could be greatly facilitated by preferred intermolecular stacking of the π-surfaces. The optical and electronic properties are not only determined by the core aromatic structure of these disk-shaped molecules, but also strongly dependent on the sidechains, which directly impact the molecular self-assembly behavior in condensed phases. Triphenylene-tris(naphthaleneimidazole) (TP-TNI) is a recently reported n-type semiconductor featuring a large π-core and branched sidechains with an electron transporting mobility reaching 10^{-4} $cm^2V^{-1}s^{-1}$. In order to further improve material performance, a detailed study is needed to understand the dependence of carrier transporting properties on both the core electronic structure and the sidechain. Here we present the detailed synthesis and characterization of a TP-TNI derivative bearing linear sidechains, which has demonstrated a field effect electron transport mobility up to 1.3×10^{-3} cm^2 V^{-1} s^{-1}. The more than one order improvement of electron transport properties over the branched side chain homologue can be correlated to ordered twisted packing in the thin film, as revealed by *in situ* variable temperature grazing incidence wide-angle X-ray scattering (GIWAXS) studies. In-depth theoretical understanding of the frontier orbitals, reorganization energies and charge transfer integrals of TP-TNI molecules have provided further insight into the relationship between molecular stacking geometry and charge transporting properties.

INTRODUCTION

Disk-shaped molecules containing polycyclic aromatic cores represent one class of organic semiconductors with controllable self assembly and anisotropic transporting properties.[1-3] The strong intermolecular interactions between the large planar aromatic surfaces incur favorable tendency for such molecules to stack into one-dimensional (1D) columns, which can serve as the preferred charge carrier transporting pathway through inter-stack hopping. In the solid state, these 1D columns can further organize into two dimensional suprastructures.[4] Both the long-range order in these suprastructures and the orientation of the columns play a key role in determining the electronic properties of these organic semiconductors. Depending on the nature of the aromatic core, these disk-shaped materials can be either hole-transporting, electron transporting, or ambipolar. There are abundant examples of hole-transporting disk-shaped molecules, however these with good electron-transporting properties remain underdeveloped and thus require much more research endeavor.[3] From a molecular design point of view, the nature of the charge carriers could be empirically engineered by adjusting the electron density of the aromatic unit. Introduction of electron deficient nitrogen atoms[5-8] onto the aromatic core has been an effective method in endowing *n*-type characteristics. An emerging trend in recent *n*-type disk-shaped molecules is manifested in the ladder-conjugated molecules containing rylene imide building blocks.[9-13] Previously we have demonstrated that fusing a triphenylene core with three aroyleneimide imidazoles gave rise to novel *n*-type disk-shaped molecules with enhanced optical properties and well-positioned frontier orbitals. The TP-TNI-BC15 molecule (Scheme 1), which is based on a naphthaleneimide-fused trimeric core and bears three branched sidechains,[12] has displayed a decent field effect electron mobility of 1.3×10^{-4} cm^2 V^{-1} s^{-1} based on solution processed organic field effect transistor (OFET) devices. While promising, there is clearly more

room for fine tuning the charge transporting characteristics, which calls for both theoretical understanding and synthetic modification of molecular details that concern both the aromatic core and the sidechains. On the one hand, a detailed study on the electronic structure of the large π core of TP-TNI, and the implication on the reorganization energy and charge transfer integral would provide a better understanding of the relationship between intracolumnar stacking and charge transport.[14] On the other hand, experimental alteration of the sidechain structures could influence the solid state packing geometry and subsequently charge transporting properties.[15]

In this work, we address the two aspects of the TP-TNI system by (a) experimentally introducing linear sidechains in place of the original branched ones to investigate the impact on the thermotropic solid-state packing behavior and charge transporting properties in thin film transistors, and (b) theoretical modeling focusing on the aromatic core of TP-TNI, including detailed analysis of frontier orbital energy, optical transitions and reorganization energy of single molecules, and charge transfer integral of dimers. The introduction of linear sidechains has led to significantly improved OFET device characteristics, which can be correlated with the structural changes revealed by *in situ* GIWAXS studies. Theoretical modeling provides further in-depth understanding of the relationship between molecular structures and the related optoelectronic properties.

RESULTS AND DISCUSSION

TP-TNI synthesis and characterization. TP-TNI derivative containing linear $C_{12}H_{25}$ side chains, named as TP-TNI-C12, was synthesized by the condensation reaction between hexaaminotriphenylene and the corresponding monoanhydride bearing a n-dodecyl chain.[12] TP-TNI-C12 was obtained as an inseparable statistic mixture of *cis*- (symmetric) and *trans*-

(asymmetric) isomers with a ratio of 1:3, both having good solubility in solvents such as CH_2Cl_2 and $CHCl_3$. Thermogravimetric analysis (TGA) indicated high thermal stability of TP-TNI-C12 above 450 ºC (Figure S1). Corresponding differential scanning calorimmetry (DSC) studies revealed no thermal transitions within the range between 20 ºC and 350 ºC, and thus the lack of liquid crystalline mesophase (Figure S2). UV-vis spectroscopic studies of the TP-TNI-C12 solution indicated a broad lowest frequency absorption peak spanning 430 and 710 nm, with a peak centered at 515 nm (ε = 23900 M^{-1} cm^{-1}) and a shoulder peak at 607 nm (ε = 12100 M^{-1} cm^{-1}). In comparison, the branched TP-TNI-BC15 also displays a broad but narrower absorption peak that extends only to 650 nm and peaks at 515 nm (ε = 25600 M^{-1} cm^{-1}) (Figure 1). Both compounds show even broader absorption spectra when casted into thin films. An absorption feature at around 607 nm emerges in the thin film of TP-TNI-BC15, and for TP-TNI-C12, the absorption in the corresponding spectrum became more intensified. These results suggest that the absorption feature at around 607 nm is a result of molecular aggregation. The contrast in solution suggests that the TP-TNI molecules with linear side chains are significantly more aggregated than the branch-chain substituted one. When going from solution to thin films, molecular aggregation is promoted in both cases, while the relatively higher intensity at 607 nm in TP-TNI-C12 correlates well with its stronger aggregation tendency. An optical bandgap of 1.86 eV can be estimated for TP-TNI-C12 from the solution absorption onset. The lowest occupied molecular orbital (LUMO) energy level was estimated to be -3.7 eV from cyclic voltammetric studies (Figure S3). The highest occupied molecular orbital (HOMO) energy level was thus determined to be -5.6 eV based on the optical bandgap. The strong tendency of molecular aggregation was also evidenced by the formation of long fibril structures upon addition of methanol into the $CHCl_3$ solution of TP-TNI-C12 (Figure 2).

Scheme 1. The isomeric structures of TP-TNI molecules bearing linear (TP-TNI-C12) and branched sidechains (TP-TNI-BC15). The black arrow indicates closer atomic contacts in the *trans*-isomer.

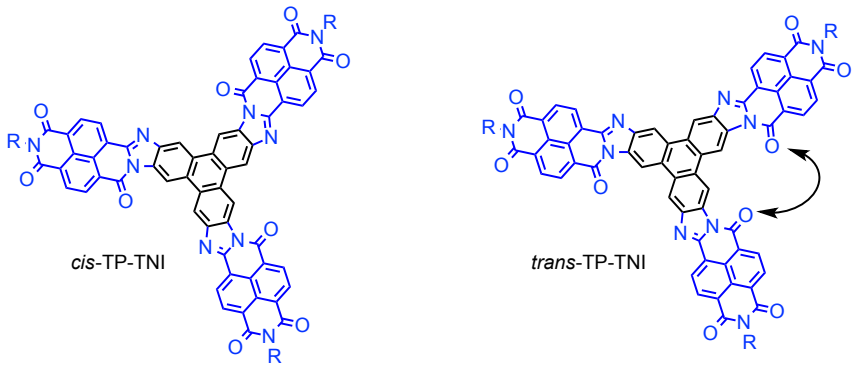

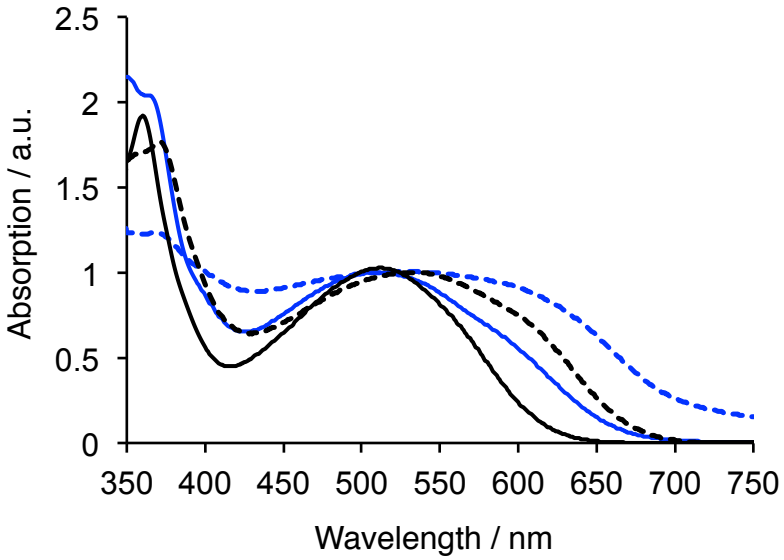

Figure 1. Normalized UV-vis spectra of TP-TNI-BC15 and TP-TNI-C12 from their $CHCl_3$ solutions and thin films (TP-TNI-BC15, black lines; TP-TNI-C12, blue lines; solution, solid lines; thin film, dotted lines). The thin films for TP-TNI-BC15 and TP-TNI-C12 are made by spincast and dropcast, respectively. The latter shows scattering due to film inhomogeneity.

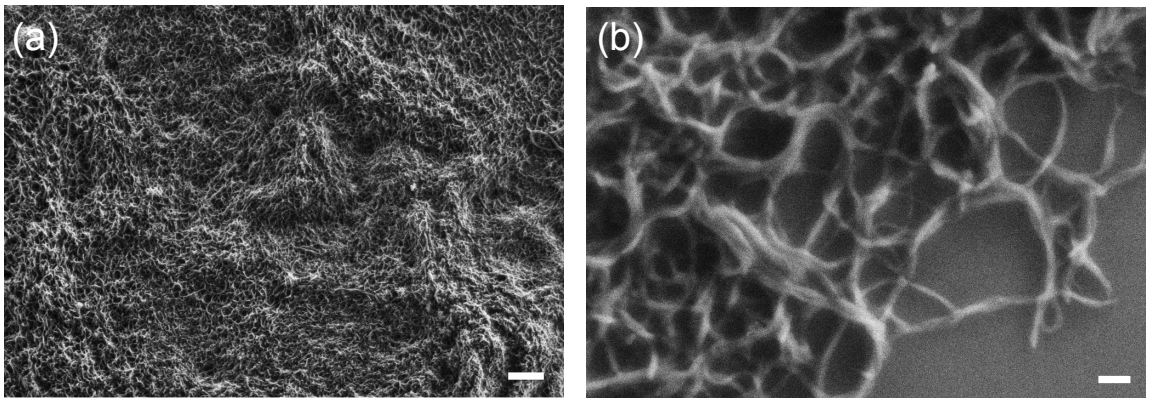

Figure 2. SEM of TP-TNI-C12 nanofibers in (a) larger and (b) smaller areas. Scale bars are 2 μm and 0.2 μm in (a) and (b), respectively.

Charge transport properties. Charge transport properties of TP-TNI-C12 were evaluated in thin film FETs, using the bottom gate/top contact OFET configuration with octadecyltrichlorosilane (OTS)-modified SiO_2 as the dielectric layer. Gold (Au) was used as the source/drain electrodes, and the scratched *n*-doped Si worked as the gate electrode. TP-TN-C12 films were prepared by drop-casting 100 μL dichloromethane solution of active materials (0.1 mg mL^{-1}) onto OTS-SiO_2 as films prepared by spincasting gave poor surface coverage. The optical image (Figure S4), revealed that dropcasted films were not uniform, but gave much better surface coverage of active layer, which allowed electron mobility measurement using FET device architecture. It suggests that the measured mobilities should be deemed as lower bound of the materials transport properties, which could be improved through optimized thin film deposition process. When thermal treatment was applied, the thin films were heated at 120 ºC for 30 min, followed by slow cooling to room temperature in 1 h. All the devices displayed typical n-type transporting behavior, with output and transfer characteristics summarized and compared in Figure 3 and Table 1. Devices from as-cast thin films showed an average and a highest electron mobility (μ) of 4.3×10^{-4} cm^2 V^{-1} s^{-1} and 6.7×10^{-4} cm^2 V^{-1} s^{-1}, respectively. Upon thermal

annealing, the average electron mobility increased to 1.0×10^{-3} cm^2 V^{-1} s^{-1}, with the highest reaching 1.3×10^{-3} cm^2 V^{-1} s^{-1}. The on/off ratios of both devices were on the order of 10^4, while the V_{th} of annealed devices decreased from 18 V to 12 V, an indication of less charge trapping sites in the annealed thin films. The electron mobility of TP-TNI-C12 is one order higher than that of the TP-TNI-BC15 (see Table 1),[12] suggesting that the linear chains facilitate intermolecular organizations that are more favorable for charge transport. This is in accordance with the different steric effects imposed by the side chains, as branching in side chains lead to intracolumnar stacking with different twist angles and π-stacking distances that are detrimental to charge transport. The enhanced electron mobility from thermal annealing also suggested improved molecular ordering upon thermal treatment, although the featureless DSC curve failed to reveal any thermotropic behavior in the thin film. We have thus turned to other alternative characterization method to probe solid-state molecular reorganizations.

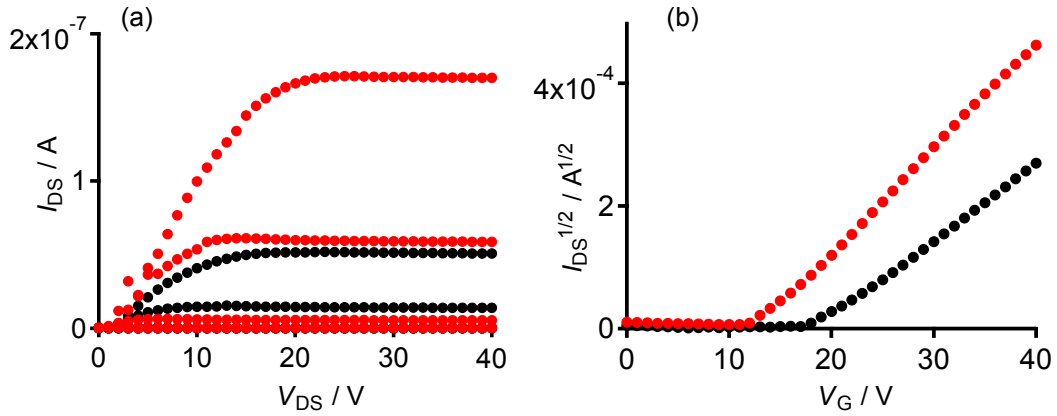

Figure 3. (a) Output and (b) transfer characteristics of OFETs based on TP-TNI-C12 thin films before (black) and after (red) thermal treatment. Output curves were recorded within the range of V_{DS} as -5 V to 40 V under V_{GS} = 0, 10, 20, 30, 40 V. Transfer characteristics were recorded under V_{DS} = 40 V.

Table 1. Summary of OFET characteristics of TP-TNI molecules.

Compound	Film deposition	$\mu_e^{avg,a}$ $cm^2 V^{-1} s^{-1}$	$\mu_e^{dev,a}$ $cm^2 V^{-1} s^{-1}$	μ_e^{max} $cm^2 V^{-1} s^{-1}$	V_{th} V	I_{On}/I_{Off}
TP-TNI-C12	As cast	4.3×10^{-4}	1.8×10^{-7}	6.7×10^{-4}	18	10^4
TP-TNI-C12	Annealed[b]	1.0×10^{-3}	1.6×10^{-7}	1.3×10^{-3}	12	10^4
TP-TNI-BC15	As cast	2.0×10^{-5}	9.7×10^{-6}	2.9×10^{-5}	18	10^4
TP-TNI-BC15[c]	Annealed[b]	8.5×10^{-5}	4.1×10^{-5}	1.3×10^{-4}	8	10^4

[a]average of 2-8 pixels on 1-2 chips. [b]annealed at 120 ºC for 30 mins, and then slowly cooled down to room temperature. [c]from reference 9.

Thermal responsive self-Assembly of TP-TNI-C12 by *in situ* variable temperature GIWAXS studies. Synchrotron GIWAXS has been a very useful tool in providing in-plane and out-of-plane molecular packing information in thin films. In addition, *in situ* variable temperature studies could provide details of real time structural changes with better sensitivity than conventional thermal characterizations. As revealed by GIWAXS studies, TP-TNI-C12 does undergo substantial structural reorganization that corresponds to changes of both intracolumnar and intercolumnar assembly upon thermal annealing, the enthalpy changes of which probably were too small to be detected by DSC.

The GIWAXS pattern of TP-TNI-C12 thin film at room temperature displays a strong in-plane π-stacking peak with a *d* spacing of 3.50 Å (Figure 4), which appears as a strong peak at 1.79 $Å^{-1}$ in the in-plane linecut but is absent in the out-of-plane linecut (Figure 5). This localized diffraction clearly indicates that the π-stacking columns resulted from intermolecular stacking of TP-TNI-C12 molecules are laying parallel to the substrate. This preferred orientation of columns

is commensurate with the strong out-of-plane peaks, which corresponds to hexagonally packed columns with an intercolumn distance of 33 Å. This distance is larger than the column diameter defined by the aromatic core (~24 Å) but smaller than that of the columns counting both the core and fully extended peripheral groups (~52 Å), implying that there is side chain interdigitation between TP-TNI-C12 molecules from adjacent columns. The in-plane linecut also indicates a (001) peak with *d* spacing of 32.4 Å, suggesting an additional long-range period along the column attributed to the twisted columnar structure that contains ten (32.4/3.5 = 9) disk-shaped molecules. Since a rotation of roughly 120º is needed for superposition of the first and tenth molecule in one period, a rotation angle between adjacent disk-shaped molecules can be determined by 120º/9 to be around 13º. As the temperature is increased up to 357 ºC, more high order diffraction peaks appear, which suggest the rearrangement of the columns into more ordered hexagonal packing. From the stack of in-plane linecuts it is found that the π-π stacking distance increases slightly from 3.50 to 3.57 Å as the temperature increases, concomitantly the coherence length of the π-stacks also increases from 3.0 nm to 4.4 nm, indicating that at higher temperature the intramolecular stacking becomes more relaxed and the molecules have a higher tendency to form longer stacking columns. The increased coherence length at higher temperature lead to less defects states, which correlate well with the reduced threshold voltage in annealed devices. On the other hand, the intercolumnar spacing increases at elevated temperature, an indication of decreased interchain interactions between alkyl side chains. When the thin film is cooled back to 40 ºC, the high crystallinity remains as indicated by the retention of multiple diffraction peaks which can be indexed according to a hexagonal unit cell. Meanwhile both the intercolumnar spacing and the π-stacking distance decrease simultaneously, yet the number of molecules per period in the twisted columnar structure remains to be 10 (30.5/3.45 = 9).

Altogether these changes suggest that these disk-shaped molecules become more organized following thermal induced inter- and intracolumnar rearrangements, and are able to remain higher crystallinity while undergoing small lattice relaxation. The thermally enhanced intercolumnar and intracolumnar order is consistent with the significantly improved electron mobility observed in thermally annealed FET devices.

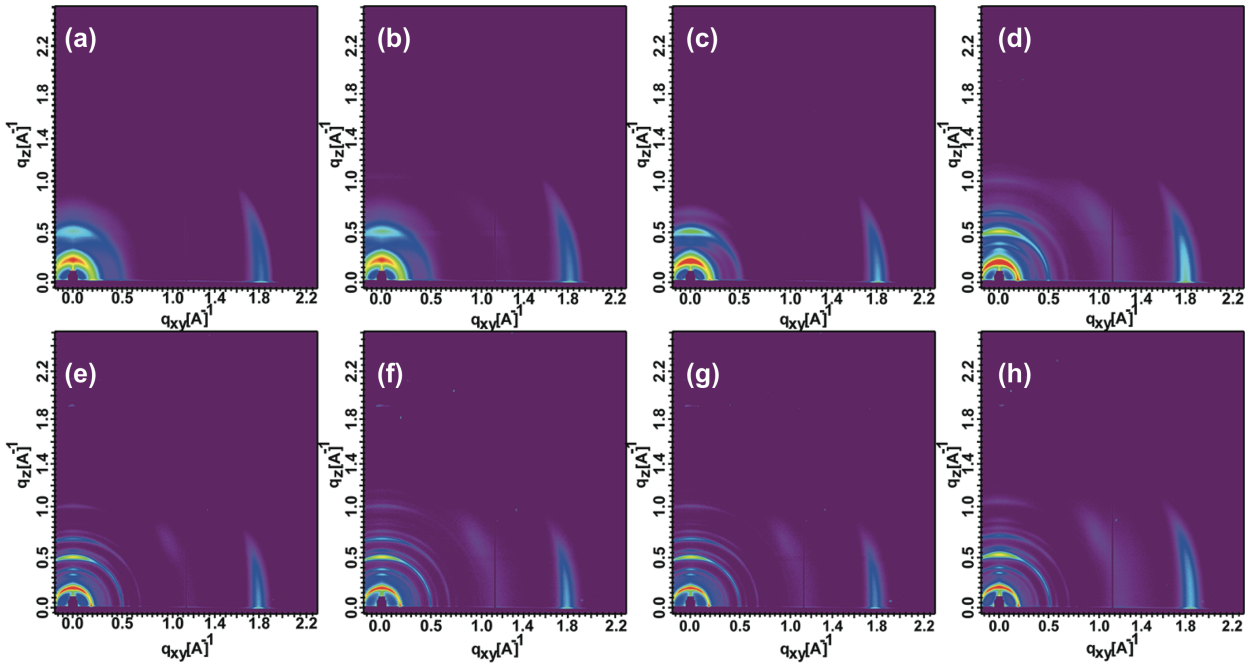

Figure 4. In-situ GIWAXS patterns of TP-TNI-C12 at different temperatures: (a) 23 ºC, (b) 131 ºC, (c) 201 ºC, (d) 256 ºC, (e) 312 ºC, (f) 356 ºC, (g) 367 ºC, (h) cooled down to 40 ºC.

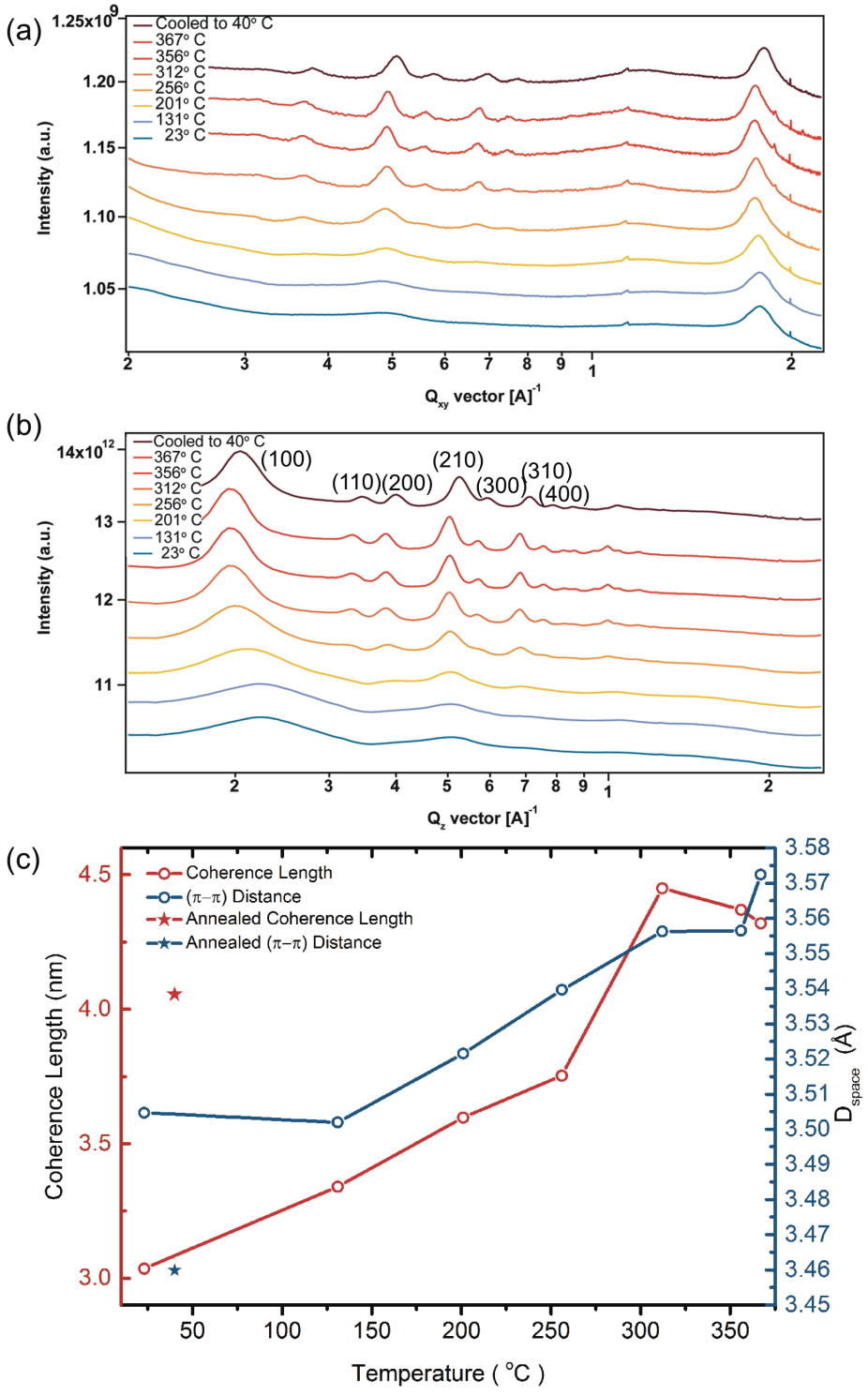

Figure 5. Stack of (a) horizontal and (b) vertical linecuts; (c) plot of the coherence length and π-π distance against temperature.

Theoretical modeling of the TP-TNI core. The electronic structures and properties of the TP-TNI core were modeled, taking into consideration of both the *cis*- and *trans*- isomers. In spite of the fact that side chains play an important role in the packing of the molecules in the columns, they have little effect on the reorganization energy and transfer integral calculations.[14,16-18] Thus, the long alkyl chains were replaced by methyl groups in the calculations to reduce the computational cost unless stated otherwise. All theoretical calculations were performed using the Gaussian09 (revision D.01) suite of programs.[19] Full geometry optimization was carried out on *cis* and *trans* isomers of TP-TNI (Scheme 1) at the Density Functional Theory (DFT) level by using the Becke's three-parameter B3LYP exchange functional[20,21] and 6-31G** basis set. The geometries of the neutral and charged, anionic and cationic, selected compounds were fully optimized in gas phase and vibrational frequencies were calculated to check that all are positive values. HOMO and LUMO frontier molecular orbitals, band gap, electron affinity and ionization potential, internal reorganization energy, transfer integral and charge mobility for holes and electrons have been calculated on the basis of density functional theory (DFT). The vertical excitation energies, oscillator strengths and configurations involved in the electronic transitions were evaluated using the ground-state optimized geometries and time-dependent density functional theory (TD-DFT) at the B3LYP/6-31** level of theory. The *cis* and *trans* isomers were modeled in $CHCl_3$ solution using the polarizable continuum model (PCM) and the linear response formalism.[22,23]

As described in the literature,[14,16,24] the charge transport within a discotic phase mainly occurs through a hopping regime. The rate of charge hopping k between two adjacent discs can be estimated to first approximation on the basis of semi-classical Marcus theory[25] according to:

$$k = \frac{4\pi^2}{h} \frac{1}{\sqrt{4\pi\lambda\kappa_B T}} t^2 \exp\left[\frac{-\lambda}{4\kappa_B T}\right] \qquad (1)$$

where the reorganization energy (λ) and the charge transfer integral (t) are the two key parameters. The charge transfer integral t for a dimer was estimated following the so-called projective method using the code *J-from-g0*.[26,27] As discussed in previous studies,[14] we will only consider the internal reorganization energy and the external contribution will be neglected. According to the hopping mechanism, the carrier mobility (μ_{hop}) can be calculated by the Einstein equation: [28]

$$\mu_{hop} = \frac{eD}{\kappa_B T} \qquad (2)$$

where T is the temperature, e is the electronic charge, k_B is the Boltzmann constant. D is charge the diffusion coefficient given by $D = 1/2\ l^2 k$ for a one-dimensional system, where only one neighbor is considered, being l the distance between molecules and k the hopping rate calculated according to equation (1).

The geometry optimizations yield planar structures for both *cis* (symmetric) and *trans* (asymmetric) isomers that have very similar total energies (Table S1). The calculated frontier orbital energies, the relative energy levels, and the frontier molecular orbital isosurfaces are illustrated in Table 2, Figure S5 and S6, respectively. The LUMO energy levels are predicted around -3.5 eV while the HOMO energy level is around -5.9 eV and -5.8 eV for the *cis* and *trans* isomer, respectively. These results are in agreement with the experimental values of -3.7 eV and -5.6 eV for the LUMO and HOMO energy levels, respectively. For both isomers, the LUMO is mainly distributed over the naphthaleneimide imidazole units whereas the HOMO is localized in

the triphenylene central core and to some extent over the peripheral arms. The vertical transitions and optical bandgaps have been calculated for both isomers in $CHCl_3$ solvent (see Table S2), which agree well with the experimental results.

Table 2. Theoretical energy parameters and reorganization energies of TP-TNI (in eV).

	HOMO	LUMO	ΔE_{H-L}	AIP	AEA	λ_+	λ_-
cis-TP-TNI	-5.90	-3.48	2.42	6.709	2.753	0.213	0.103
trans-TP-TNI	-5.82	-3.53	2.29	6.611	2.802	0.208	0.106

Table 2 also listed the adiabatic electron affinity and ionization potential along with the internal reorganization energy for holes, λ_+, and electrons, λ_-. For *n*-type materials, the electron affinity must be at least 3.0 eV to allow an efficient injection of electrons into the LUMO of the semiconductor molecules but not much higher than 4.0 eV to ensure the stability of the material at ambient conditions.[29] The predicted electron affinity for TP-TNI is around 2.8 eV and indeed very close to the threshold value,[30], which favors an efficient electron injection from the electrode and makes TP-TNI a good candidate to behave as an n-type organic semiconductor. The internal reorganization energy should be small enough for an efficient charge transport. The calculated electron reorganization energy λ_- is lower than λ_+ for both isomers of TP-TNI, favoring the creation of the negative polarons and the *n*-type character. The predicted value for λ_+ in TP-TNI (~ 0.21 eV) is higher than those calculated by Brédas *et al*.[14] for typical discotic systems, such as triphenylene (0.18 eV), hexaazatrinaphthylene (0.14 eV) and hexabenzocoronene (0.10 eV) calculated at the same level of theory.[14] On the other hand, the calculated λ_- for TP-TNI is around 0.10 eV, which are very close, or even inferior, to those

calculated for triphenylene (0.26 eV), hexaazatriphenylene (0.27 eV), hexaazatrinaphthylene (0.10 eV) and hexabenzocoronene (0.14 eV) at the same level of theory.[14] These results bode well for the excellent *n*-type characters of TP-TNI aromatic systems.

As having been reported in the literature,[14,15,31,32] the charge transport in discotic systems is highly influenced by the local arrangement of stacked π-conjugated cores. The length, type (linear/branched) and chemical structure of the side chains along with the π-conjugated core are the main parameters from a molecular point of view that chemists can combine to tailor the charge transport properties in organic semiconductors.[33-36] In spite of the fact that side chains are insulators, they play an important role in the functional properties of these materials because of the great influence on the molecular arrangement of the stacks through no-covalent interactions, which facilitates or hampers the stabilization of the columnar stacking. In order to predict the preferred orientation of the discs, the evolution of the total energy of a dimer was calculated at 10º intervals between 0º to 120º when one molecule is rotated with respect to another, with the inter-disc distance kept at 3.5 Å (Figure 6). Since TP-TNI exists as a mixture of two isomers, we take into consideration of three types of dimers, including *cis-cis* and *trans-trans* homodimers, and *cis-trans* heterodimers. Stacking geometries of these dimers are plotted at three representative rotation angles of 0º, 100º, and 120º, respectively. Figure 7 shows the energy barrier to rotate along the staking axis for all three dimers. The energies of the dimers are highest at rotation angles of 0º, which decreases significantly as the molecules rotate. A relatively flat energy well was observed between 10º and 100º, and a sharp rise occurs at 120º, clearly indicating that cofacial stacking is disfavored. Most stable arrangement was found for cores with a rotation angle of 40º (or 80º), and the *cis-trans* heterodimer has higher relative energy compared to the homodimers with respect to the cofacial stacking. In order to gain further insight

on the influence of sidechains, calculations were also carried out on the molecules containing the dodecyloxy chains. As can be seen from Figure 7, relatively flat energy wells were observed in the rotation angle range between 10° and 90° where the steric hindrance of the side chains should be minimized. The theoretical calculations confirm the stabilization of the dimer when the rotation angle between the discs is slightly twisted (15-20 degrees) with respect to the less favored cofacial orientation. This result is in agreement with the experimental twist angle of 13° from GIWAXS studies.

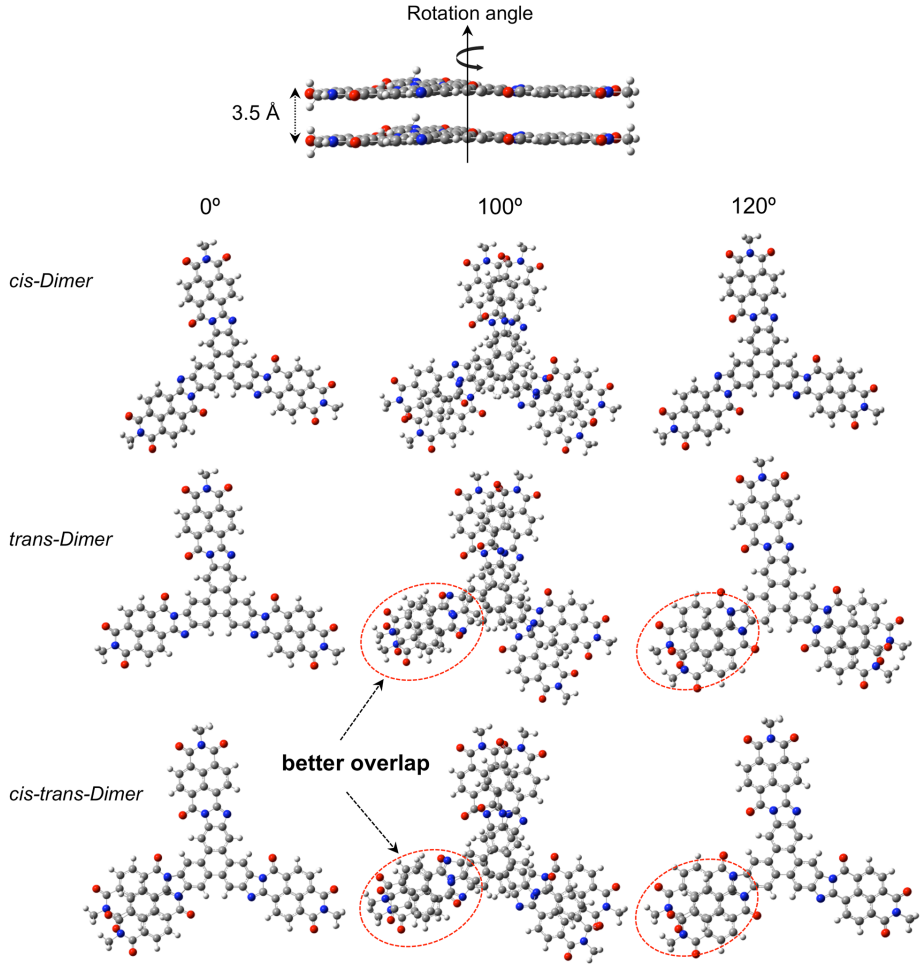

Figure 6. Schematic representation of the model stacked dimers at rotation angles of 0°, 100°, and 120°, respectively.

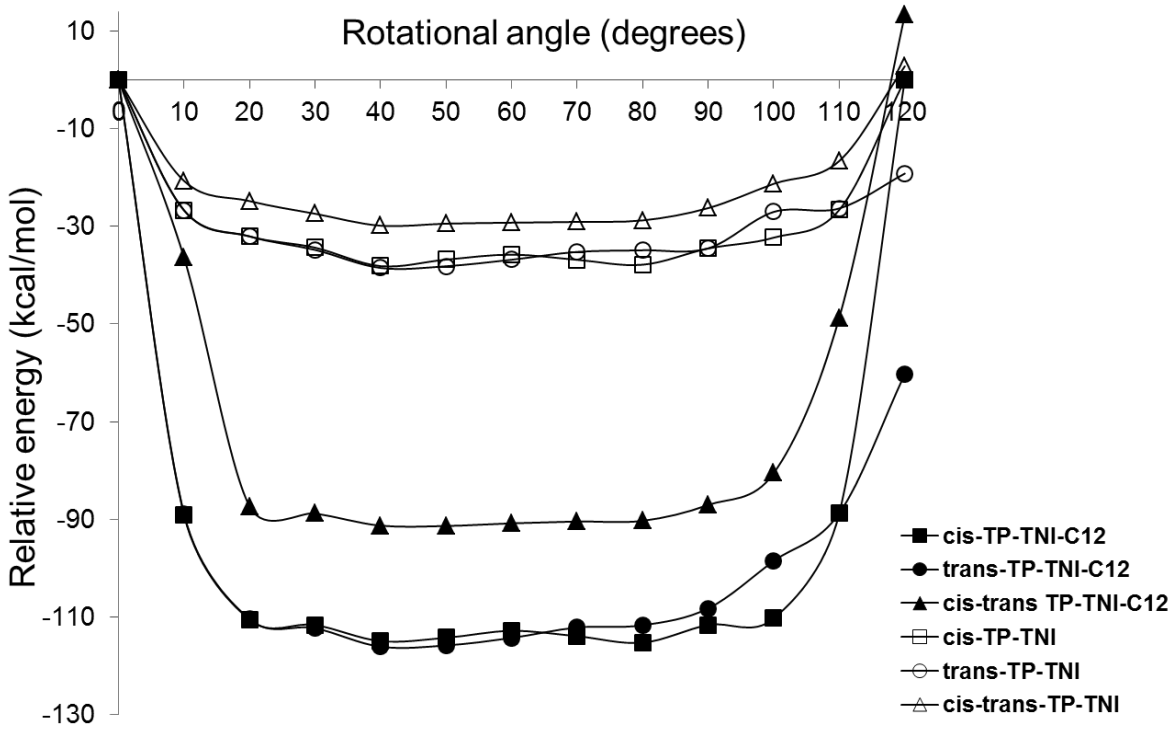

Figure 7. Relative energy of a dimer as a function of rotation angle. The solid and open symbols represent TNIs bearing methoxy and dodecyloxy sidechains, respectively.

Since the transfer integral is strongly dependent on the relative position and orientation of the neighboring discs,[32] the transfer integral for holes and electrons has thus been calculated as a function of the rotation angle from 0º to 120º for a dimer built from the optimized geometry of the monomer with the inter-disc distance kept at 3.5 Å (Figure 8 and Table S3). Not unexpectedly, calculations predict the highest values for both hole (t_+) and electron (t_-) transfer integrals (~0.3 eV) in the homodimers at 0º, which corresponds to a perfectly cofacial stacking. In the case of heterodimer, the electron transfer integral is significantly lower than the hole transfer integral, presumably due to less overlap of the imide arms where LUMO is primarily localized (Figure 6). When one molecule is rotated, a dramatic decrease of the transfer integral,

up to one order of magnitude improvement compared to the face-to-face orientation, is predicted except for the electron transfer integral of the heterodimer. In the case of homodimers, the electron transfer integral undergoes a more pronounced decrease due to the fact that the LUMO is localized in the peripheral arms. In both the *trans*-dimer and the heterodimer, a rise in electron transfer integral is predicted at a rotation angle of 100° (see Table S3 for a full list of calculated hole and electron transfer integral), which correlates with better overlap of the arms as indicated in Figure 6. This rotational angle, which is experimentally indiscernible from a 20° rotation, is close to that (~13°) derived from the scattering experiment. The calculated higher t_- compared to t_+ at this angle also corroborates with the observed electron dominant transporting behavior.

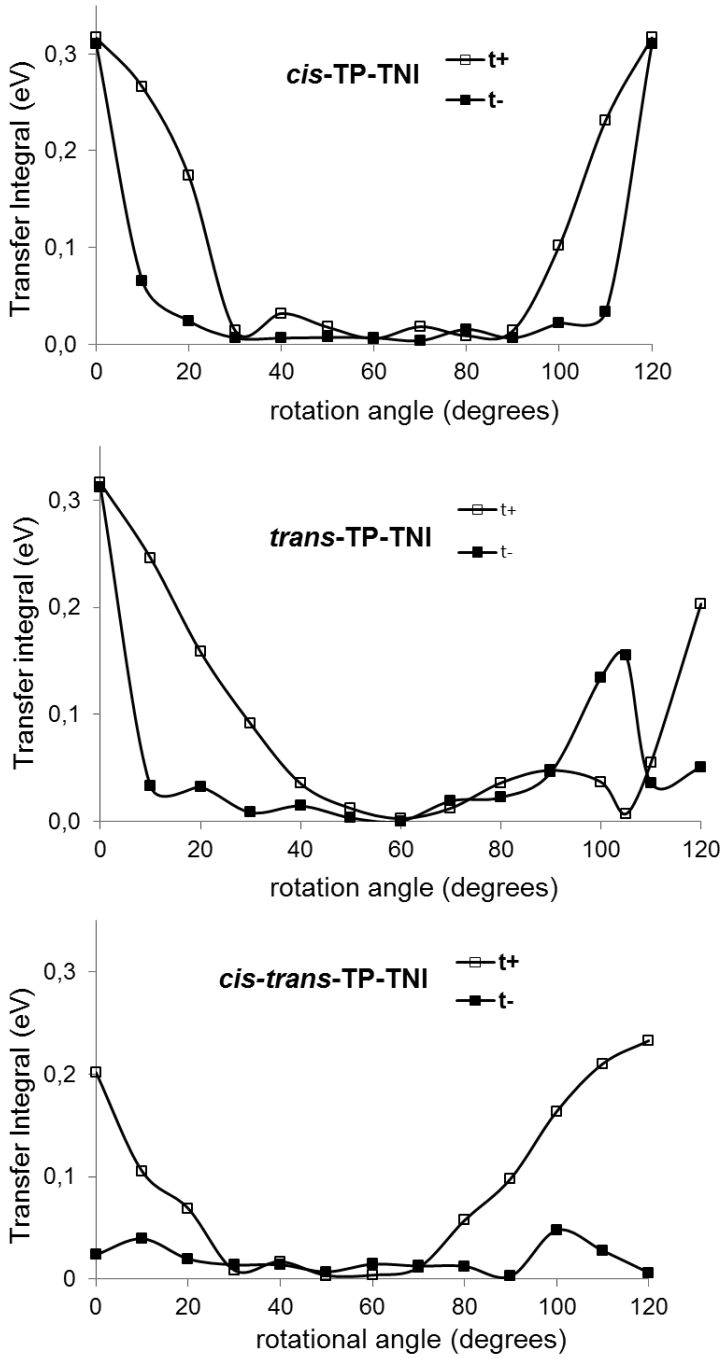

Figure 8. Hole (t_+) and electron (t_-) transfer integral for the *cis*, *trans* and *cis-trans* isomers as a function of rotation of one molecule around the stacking axis (the inter-disk distance of 3.5 Å was fixed).

DFT method has shown to be very useful to predict the main parameters involved in the charge transport process and to establish structure-property relationships. To this point, the theoretical calculations over the charge injection and charge transport properties on TP-TNI have confirmed that it has suitable intrinsic properties to behave as n-type organic semiconductor. In order to estimate the dependence of the charge mobility on the intracolumnar molecular geometry, we have calculated the charge mobility for holes (μ_+) and electrons (μ_-) of the dimers using the equation (2) that take into account both the internal reorganization energy and transfer integral values (Figure 9 and Table S3). In TP-TNI there are three different hopping pairs which have different ability for charge transport. The calculations were performed over ideal, isolated dimers; therefore the results must be taken with caution because they represent the upper limit for the charge mobility. In the real system, the charge carrier mobility is influenced by the intracolumnar disorder, domain boundaries and stack dynamics, all of which could significantly reduce the charge mobility. Also, the polarization of the surrounding medium was neglected in the calculations without considering the external reorganization energy in the Marcus equation. Thus, due to the simplicity of the theoretical model, the goal was to estimate qualitatively the impact of the rotation angle on the charge mobility on the hopping pairs. The highest carrier transport mobilities are at 0º rotation angle, when the face-to-face orientation yields electron mobility values larger than the hole ones, ~43 and 11 $cm^2V^{-1}s^{-1}$, respectively. This face-to-face stacking however is least favorable as revealed in Figure 7 and inconsistent with the experimentally determined twisted stacking geometry. As the rotation angle starts to increase, significant decrease of both carrier mobilities occurs. Since the electron transfer integral is more affected by the rotation of the molecules in comparison to the hole transfer integral, this fact is reflected in the corresponding calculated electron mobilities compared to the hole mobilities,

resulting in hole-dominant carrier transport. However, at rotation angles around 100º, electron mobility still remains significantly higher than the hole mobility for the *trans* dimer despite both being significantly reduced. Thus, theoretical calculations have shown that both the electron-dominant transport and the rotation angle calculated for the *trans-trans* dimer corroborate with these observed experimentally in TP-TNI molecules.

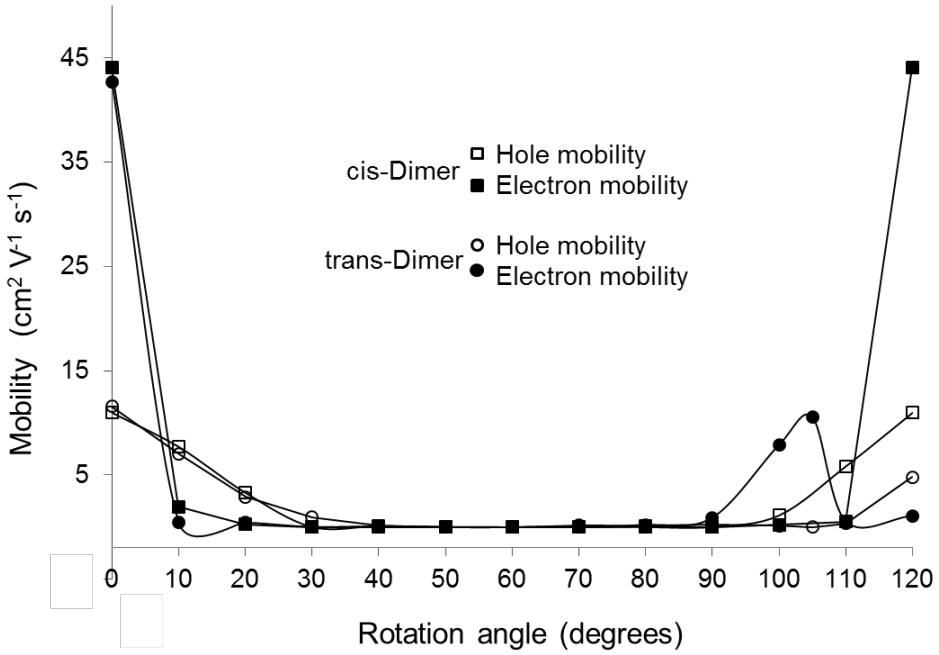

Figure 9. Calculated hole and electron transfer mobilities for *cis* and *trans* isomers as a function of rotation of one molecule around the stacking axis.

Overall, the experimental results indicate that the use of linear sidechains instead of branched ones can effectively enhance the order within thin films and correspondingly the electron transport properties. Scattering experiment suggested a twisted columnar stacking with a rotation angle around 13º. Modeling results have validated that the intracolumnar stacking deviates from the cofacial stack and favors a rotated stacking geometry. The deviation from

cofacial stacking, however, is highly detrimental for charge mobilities due to the smaller overlap of the electronic wave function of the two molecules in the dimer, and more so for electron transport mobility such that the dominant carriers become holes instead of electrons at most rotation angles. The modeling further indicates that at rotation angles of 100º and 105º (indiscernible from experimental angles of 20º and 15º) for the *trans-trans* dimer, a higher electron mobility than hole mobility is resulted. Considering that the *cis* and *trans* isomers exist in a 1:3 ratio in the statistical mixture, majority of the interfaces between two molecules within the same column would be *trans-trans*, thus it is reasonable to correlate this rotated arrangement with the experimental results. It is important to bear in mind that when choosing peripheral substituent groups for disk-shaped molecules such as TP-TNI, one needs to achieve a balanced steric demand to avoid repulsion from each other, while at the same time to minimize the twisting that is disfavored for transfer integral and inferior for charge transport.

CONCLUSIONS

We have presented a comprehensive study on an *n*-type disk-shaped TP-TNI core by both experimental validation of a sidechain engineering approach to improving charge transport and theoretical modeling of the electronic structure, packing and charge transport. The replacement of the branched sidechains to linear ones has a strong influence on the self-assembly and charge transport properties. *In situ* variable temperature GIWAXS studies have provided more details on the temperature induced changes of inter- and inra-columnar molecular organization, which correlates to more than one-order improvement of electron transporting mobility when compared to the TP-TNI bearing branched sidechains. DFT calculations on the frontier orbitals, reorganization energies, and charge transfer integrals of the TP-TNI core have provided in-depth understanding of the optoelectronic and charge-transport properties. As the charge transport in

discotic systems is influenced by the local arrangement of stacked π-conjugated cores, we have determined the evolution of the total energy of a dimer when one molecule is rotated with respect to another one. Also, the evolution of the transfer integral as a function of the rotation angle has been estimated. While a face-to-face stacking gives the highest predicted carrier transport mobilities for both electrons and holes, the cofacial arrangement is energetically disfavored. Significant differences for the predicted values were obtained depending on the rotation angle, with the twisted stacking in *trans* dimer at a rotation angle around 100º favoring electron transport. The angle-dependent carrier transporting behavior shed light on the molecular stacking geometry in TP-TNI thin films. The findings from the combined experimental and theoretical investigations are of great relevance to the future design of novel organic semiconductors based on disk-shaped aromatic systems.

ASSOCIATED CONTENT

Supporting Information. Synthesis and characterization details. Device fabrication and characterization. Computational details and modeling results. This material is available free of charge via the Internet at http://pubs.acs.org.

AUTHOR INFORMATION

Corresponding Author

yliu@lbl.gov; anavarro@ujaen.es

Author Contributions

The manuscript was written through contributions of all authors. All authors have given approval to the final version of the manuscript. ‡These authors contributed equally.

Funding Sources

US Department of Energy, Office of Basic Energy Sciences

ACKNOWLEDGMENT

Part of this work was performed as a user project at the Molecular Foundry, and X-ray studies were carried out at BL 7.3.3 at Advanced Light Source (ALS). Both the Molecular Foundry and ALS are user facilities supported through the Office of Science, Office of Basic Energy Sciences, of the U.S. Department of Energy, under Contract No. DE-AC02-05CH11231. The authors thank the financial support from Junta de Andalucía (FQM337) and the Centro de Servicios de Informática y Redes de Comunicaciones (CSIRC), Universidad de Granada, for providing the computing time. We also thank Prof. Alberto Salleo at Stanford University for helpful discussions. B.M. acknowledges the Florida State University for the financial support through the Energy and Materials Initiative.

REFERENCES

(1) Laschat, S.; Baro, A.; Steinke, N.; Giesselmann, F.; Hägele, C.; Scalia, G.; Judele, R.; Kapatsina, E.; Sauer, S.; Schreivogel, A.; Tosoni, M. Discotic Liquid Crystals: from Tailor-Made Synthesis to Plastic Electronics. *Angew. Chem. Int. Ed.* **2007**, *46*, 4832-4887.

(2) Sergeyev, S.; Pisula, W.; Geerts, Y. H. Discotic Liquid Crystals: a New Generation of Organic Semiconductors. *Chem. Soc. Rev.* **2007**, *36*, 1902-1929.

(3) Wöhrle, T.; Wurzbach, I.; Kirres, J.; Kostidou, A.; Kapernaum, N.; Litterscheidt, J.; Haenle, J. C.; Staffeld, P.; Baro, A.; Giesselmann, F.; Laschat, S. Discotic Liquid Crystals. *Chem. Rev.* **2016**, *116*, 1139-1241.

(4) Koshkakaryan, G.; Jiang, P.; Altoe, V.; Cao, D.; Klivansky, L. M.; Zhang, Y.; Chung, S.; Katan, A.; Martin, F.; Salmeron, M.; Ma, B.; Aloni, S.; Liu, Y. Multilayered Nanofibers from Stacks of Single-Molecular Thick Nanosheets of Hexakis(Alkoxy)Triphenylenes. *Chem. Commun*. **2010**, *46*, 8579-8581.

(5) Segura, J. L.; Juarez, R.; Ramos, M.; Seoane, C. Hexaazatriphenylene (Hat) Derivatives: from Synthesis to Molecular Design, Self-Organization and Device Applications. *Chem. Soc. Rev*. **2015**, *44*, 6850-6885.

(6) Li, J.; Zhang, Q. Linearly Fused Azaacenes: Novel Approaches and New Applications Beyond Field-Effect Transistors (FETs). *ACS Appl. Mater. Interfaces* **2015**, *7*, 28049-28062.

(7) Bunz, U. H. F. The Larger Linear *N*-Heteroacenes. *Acc. Chem. Res*. **2015**, *48*, 1676-1686.

(8) Stępień, M.; Gońka, E.; Żyła, M.; Sprutta, N. Heterocyclic Nanographenes and Other Polycyclic Heteroaromatic Compounds: Synthetic Routes, Properties, and Applications. *Chem. Rev*. **2017**, *117*, 3479-3716.

(9) Xie, Y.; Zhang, X.; Xiao, Y.; Zhang, Y.; Zhou, F.; Qi, J.; Qu, J. Fusing Three Perylenebisimide Branches and a Truxene Core into a Star-Shaped Chromophore with Strong Two-Photon Excited Fluorescence and High Photostability. *Chem. Commun*. **2012**, *48*, 4338-4340.

(10) Zhao, Z.; Xiao, Y.; Zhang, Y.; Wang, H. Fusion of Perylene Bisimides and Hexaazatriphenylene into a Star-Shaped Ladder Conjugated *n*-Type Semiconductor. *RSC Adv*. **2013**, *3*, 21373-21376.

(11) Zhang, Y.; Chen, L.; Zhang, K.; Wang, H.; Xiao, Y. A Soluble Ladder-Conjugated Star-Shaped Oligomer Composed of Four Perylene Diimide Branches and a Fluorene Core: Synthesis and Properties. *Chem. Eur. J.* **2014**, *20*, 10170-10178.

(12) Zhang, Y.; Hanifi, D.; Alvarez, S.; Antonio, F.; Pun, A.; Klivansky, L. M.; Hexemer, A.; Ma, B.; Liu, Y. Charge Transport Anisotropy in *n*-Type Disk-Shaped Triphenylene-Tris(Aroyleneimidazole)s. *Org. Lett.* **2011**, *13*, 6528-6531.

(13) Zhang, Y.; Hanifi, D.; Lim, E.; Chourou, S.; Alvarez, S.; Pun, A.; Hexemer, A.; Ma, B.; Liu, Y. Enhancing the Performance of Solution-Processed *n*-Type Organic Field-Effect Transistors by Blending with Molecular "Aligners". *Adv. Mater.* **2014**, *26*, 1223-1228.

(14) Lemaur, V.; da Silva Filho, D. A.; Coropceanu, V.; Lehmann, M.; Geerts, Y.; Piris, J.; Debije, M. G.; van de Craats, A. M.; Senthilkumar, K.; Siebbeles, L. D. A.; Warman, J. M.; Brédas, J.-L.; Cornil, J. Charge Transport Properties in Discotic Liquid Crystals: A Quantum-Chemical Insight into Structure–Property Relationships. *J. Am. Chem. Soc.* **2004**, *126*, 3271-3279.

(15) Pisula, W.; Feng, X.; Müllen, K. Tuning the Columnar Organization of Discotic Polycyclic Aromatic Hydrocarbons. *Adv. Mater.* **2010**, *22*, 3634-3649.

(16) Said, S. M.; Mahmood, M. S.; Daud, M. N.; Mohd Sabri, M. F.; Sairi, N. A. Structure-Electronics Relations of Discotic Liquid Crystals from a Molecular Modelling Perspective. *Liq. Cryst.* **2016**, 2092-2113.

(17) Nithya, R.; Senthilkumar, K. Theoretical Studies on Charge Transport and Optical Properties of Tris (*N*-Saclicylideneanilines). *RSC Adv.* **2014**, *4*, 25969-25982.

(18) Demenev, A.; Eichhorn, S. H.; Taerum, T.; Perepichka, D. F.; Patwardhan, S.; Grozema, F. C.; Siebbeles, L. D.; Klenkler, R. Quasi Temperature Independent Electron Mobility in Hexagonal Columnar Mesophases of an H-Bonded Benzotristhiophene Derivative. *Chem. Mater.* **2010**, *22*, 1420-1428.

(19) Frisch, M. J.; Trucks, G. W.; Schlegel, H. B.; Scuseria, G. E.; Robb, M. A.; Cheeseman, J. R.; Scalmani, G.; Barone, V.; Mennucci, B.; Petersson, G. A.; Nakatsuji, H.; Caricato, M.; Li, X.; Hratchian, H. P.; Izmaylov, A. F.; Bloino, J.; Zheng, G.; Sonnenberg, J. L.; Hada, M.; Ehara, M.; Toyota, K.; Fukuda, R.; Hasegawa, J.; Ishida, M.; Nakajima, T.; Honda, Y.; Kitao, O.; Nakai, H.; Vreven, T.; Montgomery, J. A., Jr.; Peralta, J. E.; Ogliaro, F.; Bearpark, M.; Heyd, J. J.; Brothers, E.; Kudin, K. N.; Staroverov, V. N.; Kobayashi, R.; Normand, J.; Raghavachari, K.; Rendell, A.; Burant, J. C.; Iyengar, S. S.; Tomasi, J.; Cossi, M.; Rega, N.; Millam, J. M.; Klene, M.; Knox, J. E.; Cross, J. B.; Bakken, V.; Adamo, C.; Jaramillo, J.; Gomperts, R.; Stratmann, R. E.; Yazyev, O.; Austin, A. J.; Cammi, R.; Pomelli, C.; Ochterski, J. W.; Martin, R. L.; Morokuma, K.; Zakrzewski, V. G.; Voth, G. A.; Salvador, P.; Dannenberg, J. J.; Dapprich, S.; Daniels, A. D.; Farkas, Ö.; Foresman, J. B.; Ortiz, J. V.; Cioslowski, J.; Fox, D. J. Gaussian 09, Revision D. 01; Gaussian, Inc., Wallingford CT: 2009.

(20) Becke, A. D. Density-Functional Thermochemistry. III. The Role of Exact Exchange. *J. Chem. Phys.* **1993**, *98*, 5648-5652.

(21) Lee, C.; Yang, W.; Parr, R. G. Development of the Colle-Salvetti Correlation-Energy Formula into a Functional of the Electron Density. *Phys. Rev. B* **1988**, *37*, 785-789.

(22) Cammi, R.; Mennucci, B.; Tomasi, J. Fast Evaluation of Geometries and Properties of Excited Molecules in Solution: A Tamm-Dancoff Model with Application to 4-Dimethylaminobenzonitrile. *J. Phys. Chem. A* **2000**, *104*, 5631-5637.

(23) Cossi, M.; Barone, V. Time-Dependent Density Functional Theory for Molecules in Liquid Solutions. *J. Chem. Phys.* **2001**, *115*, 4708-4717.

(24) Sanyal, S.; Manna, A. K.; Pati, S. K. Effect of Imide Functionalization on the Electronic, Optical, and Charge Transport Properties of Coronene: A Theoretical Study. *J. Phys. Chem. C* **2013**, *117*, 825-836.

(25) Marcus, R. A. Electron Transfer Reactions in Chemistry. Theory and Experiment. *Rev. Mod. Phys.* **1993**, *65*, 599.

(26) Baumeier, B.; Kirkpatrick, J.; Andrienko, D. Density-Functional Based Determination of Intermolecular Charge Transfer Properties for Large-Scale Morphologies. *Phys. Chem. Chem. Phys.* **2010**, *12*, 11103-11113.

(27) Kirkpatrick, J. An Approximate Method for Calculating Transfer Integrals Based on the Zindo Hamiltonian. *Inter. J. Quantum Chem.* **2008**, *108*, 51-56.

(28) Pope, M.; Swenberg, C. E. Electronic Processes in Organic Crystals and Polymers; Oxford University Press on Demand, 1999.

(29) Newman, C. R.; Frisbie, C. D.; da, S. F. D. A.; Bredas, J.-L.; Ewbank, P. C.; Mann, K. R. Introduction to Organic Thin Film Transistors and Design of *n*-Channel Organic Semiconductors. *Chem. Mater.* **2004**, *16*, 4436-4451.

(30) Chang, Y.-C.; Kuo, M.-Y.; Chen, C.-P.; Lu, H.-F.; Chao, I. On the Air Stability of *n*-Channel Organic Field-Effect Transistors: A Theoretical Study of Adiabatic Electron Affinities of Organic Semiconductors. *J. Phys. Chem. C* **2010**, *114*, 11595-11601.

(31) Chen, X.-K.; Zou, L.-Y.; Guo, J.-F.; Ren, A.-M. An Efficient Strategy for Designing *n*-Type Organic Semiconductor Materials—Introducing a Six-Membered Imide Ring into Aromatic Diimides. *J. Mater. Chem.* **2012**, *22*, 6471-6484.

(32) Feng, X.; Marcon, V.; Pisula, W.; Hansen, M. R.; Kirkpatrick, J.; Grozema, F.; Andrienko, D.; Kremer, K.; Mullen, K. Towards High Charge-Carrier Mobilities by Rational Design of the Shape and Periphery of Discotics. *Nat. Mater.* **2009**, *8*, 421-426.

(33) Pisula, W.; Tomović, Ž.; Simpson, C.; Kastler, M.; Pakula, T.; Müllen, K. Relationship between Core Size, Side Chain Length, and the Supramolecular Organization of Polycyclic Aromatic Hydrocarbons. *Chem. Mater.* **2005**, *17*, 4296-4303.

(34) Andrienko, D.; Marcon, V.; Kremer, K. Atomistic Simulation of Structure and Dynamics of Columnar Phases of Hexabenzocoronene Derivatives. *J. Chem. Phys.* **2006**, *125*, 124902.

(35) Kirres, J.; Schmitt, K.; Wurzbach, I.; Giesselmann, F.; Ludwigs, S.; Ringenberg, M.; Ruff, A.; Baro, A.; Laschat, S. Tuning Liquid Crystalline Phase Behaviour in Columnar Crown Ethers by Sulfur Substituents. *Org. Chem. Front.* **2017**, *4*, 790-803.

(36) Kirres, J.; Knecht, F.; Seubert, P.; Baro, A.; Laschat, S. δ-Methyl Branching in the Side Chain Makes the Difference: Access to Room-Temperature Discotics. *ChemPhysChem* **2016**, *17*, 1159-1165.

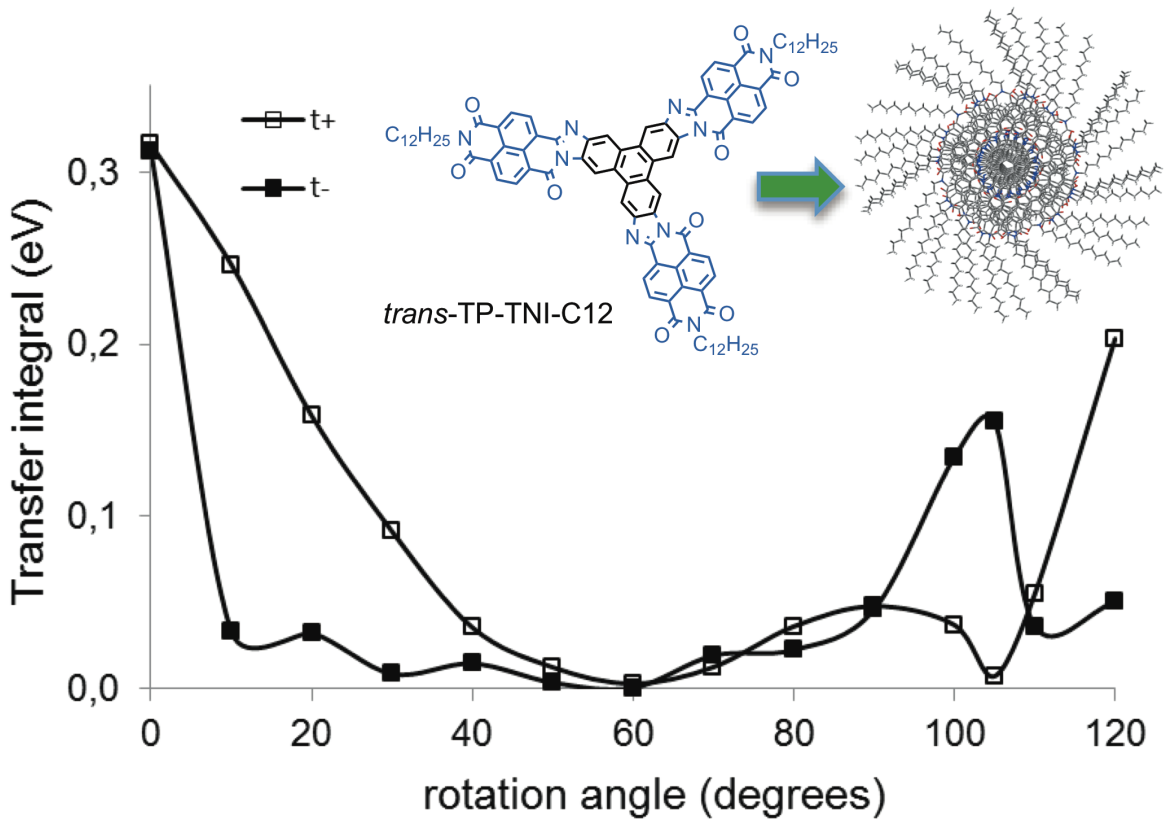
t+
t-
Transfer integral (eV)
0,3
0,2
0,1
0,0
0
20
40
60
80
100
120
rotation angle (degrees)
trans-TP-TNI-C12
C12H25